



## Optimizing HBr-Br<sub>2</sub>-H<sub>2</sub>O Etchants to Form Low Defect Regrowth Interfaces for Highly Reliable InGaAsP/InP Buried-Heterostructure Lasers

K. Shinoda,<sup>z</sup> A. Taike, H. Sato, and H. Uchiyama

Hitachi, Limited, Central Research Laboratory, Kokubunji, Tokyo 185-8601, Japan

We have obtained a tenfold improvement in the reliability of InGaAsP/InP buried heterostructure laser diodes having a dry-etched mesa structure by optimizing the composition of a HBr-Br<sub>2</sub>-H<sub>2</sub>O etchant to produce smooth mesa sidewalls, thus reducing the number of defects at regrowth interfaces. The optimal etchant, which has a composition in the range from 0.30 M HBr/0.022 M Br<sub>2</sub> to 0.50 M HBr/0.020 M Br<sub>2</sub>, etches both the InP(T10) cladding layers and the InGaAsP(T10) multi-quantum-well active layer at the same rate. We propose a simple model of the HBr-Br<sub>2</sub>-H<sub>2</sub>O etching process that is consistent with the observed etching characteristics. We found that the etching rate was controlled by the diffusion of Br<sub>2</sub> molecules, which act as oxidizing agents.

© 2003 The Electrochemical Society. [DOI: 10.1149/1.1535912] All rights reserved.

Manuscript submitted March 11, 2002; revised manuscript received June 3, 2002. Available electronically January 3, 2003.

To achieve highly reliable operation of buried-heterostructure laser diodes (BHLDs), which are vital components of optical transmission systems,<sup>1,2</sup> we must reduce the number of defects at regrowth interfaces around the mesa structures formed by dry etching followed by wet chemical etching. However, conventional wet chemical etching produces faceted mesa sidewalls because of the difference in etching rate between InP cladding layers and the InGaAsP multi-quantum-well (MQW) active layer as well as between various different crystal planes.<sup>3</sup> These faceted mesa sidewalls disrupt the uniformity of growth, so defects are formed during epitaxial regrowth. Therefore, the lasing characteristics of BHLDs gradually worsen during operation as the number of defects at the regrowth interfaces increases. Finding a wet chemical etchant that produces smooth mesa sidewalls is thus very important.

In this paper, we report on an investigation of wet chemical etchants used for etching dry-etched mesa structures. We started by examining the mechanisms by which various etchants act on InP/InGaAsP materials and chose HBr-Br<sub>2</sub>-H<sub>2</sub>O solutions as the most suitable etchants for obtaining smooth mesa sidewalls. We found that the etching characteristics depended on the solution's composition, so we were able to find the best HBr-Br<sub>2</sub>-H<sub>2</sub>O etchant composition for producing smooth mesa sidewalls. We also propose a simple model of this etching process; its predictions agree well with experimental results. Although a HBr-Br<sub>2</sub>-H<sub>2</sub>O etchant was used to etch the InGaAsP/InP mesa structure in an earlier study, the sidewalls of the resulting mesa were rough and there was a bump on each side of the MQW active layer.<sup>3</sup> The present study thus represents the first time that smooth mesa sidewalls have been formed by using a HBr-Br<sub>2</sub>-H<sub>2</sub>O etchant that was compositionally optimized to etch InP and InGaAsP at the same rate. This etchant suppressed the generation of defects at the regrowth interfaces and improved the reliability of the BHLDs.

### Experimental

**Choice of etchant system.**—Wet-etching profiles are strongly affected by whether the dissolution rate is diffusion controlled or kinetically controlled. Whereas kinetically controlled dissolution tends to produce faceted surfaces because the dissolution rate depends on the crystal plane and the composition of the material being etched, diffusion-controlled dissolution is more likely to produce smooth surfaces. This is because the rate-determining process in diffusion-controlled etching is the arrival of etchants at solid surfaces, so any differences in reaction rate that may exist for various crystal planes

and compositions do not affect the etching rate. Therefore, diffusion-controlled etchants are preferable for producing smooth mesa profiles.

Among the many systems for etching InP/InGaAsP that have been presented to date,<sup>3,4</sup> ones that contain bromine tend to be diffusion controlled. We therefore chose to examine HBr-H<sub>2</sub>O<sub>2</sub>-H<sub>2</sub>O and HBr-Br<sub>2</sub>-H<sub>2</sub>O. These are composed of an acid (HBr), an oxidizing agent (H<sub>2</sub>O<sub>2</sub> or Br<sub>2</sub>), and water. Thus, their etching processes are considered to consist of surface oxidation by the oxidizing agent, followed by the dissolution of the oxides in the presence of the oxonium ions produced by acids diluted in water.

We examined the relative stability of the two etchants by evaluating their etching rates for InP(001) as a function of time after the solution was mixed (Fig. 1). Here the etching rate represents a rough estimate of the initial rate of etching. In this paper, it was calculated by measuring the etched depth of the samples after they had been etched in the solution for 2 min. It is difficult to obtain a precise value for diffusion-limited etching because the etched depth does not increase linearly with time.

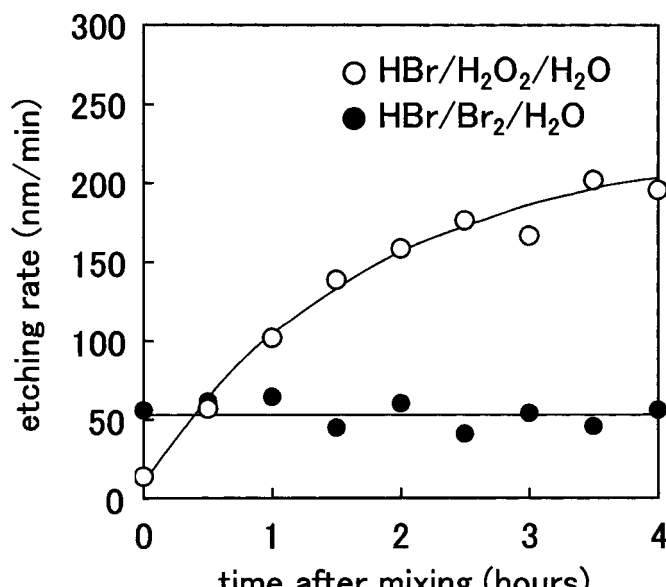


**Figure 1.** Etching rate of InP(001) vs. time after mixing each solution: (○) HBr-H<sub>2</sub>O<sub>2</sub>-H<sub>2</sub>O etchant (0.55 M HBr, 0.19 M H<sub>2</sub>O<sub>2</sub>), (●) HBr-Br<sub>2</sub>-H<sub>2</sub>O etchant (1.5 M HBr, 0.01 M Br<sub>2</sub>).

<sup>z</sup> E-mail: shinoda@crl.hitachi.co.jp

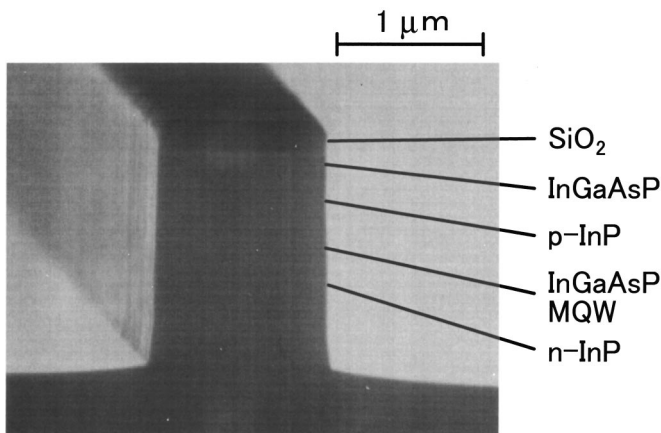


Figure 2. SEM cross-sectional image of a dry-etched mesa.

The etching rate in  $\text{HBr}-\text{H}_2\text{O}_2-\text{H}_2\text{O}$  was negligible immediately after mixing but increased substantially over time. The explanation for this is as follows.  $\text{H}_2\text{O}_2$  did not act as an oxidizing agent because  $\text{HBr}-\text{H}_2\text{O}_2-\text{H}_2\text{O}$  hardly etched InP. As time proceeded, however,  $\text{H}_2\text{O}_2$  oxidized  $\text{Br}^-$  ions to produce  $\text{Br}_2$  which did act as an oxidizing agent. This is because the standard redox potential for  $\text{H}_2\text{O}_2$  (1.763 V) is higher than that for  $\text{Br}^-$  (1.087 V).<sup>5</sup> This explanation was confirmed by the observed color of the solution, which gradually changed from colorless to red, the color of bromine. Therefore, we do not consider  $\text{HBr}-\text{H}_2\text{O}_2-\text{H}_2\text{O}$  to have good reproducibility in etching of InP and InGaAsP. Consequently, hereafter, we only discuss the  $\text{HBr}-\text{Br}_2-\text{H}_2\text{O}$  etchant system.

**Procedure.**—The dependence of the etching rate of  $\text{InP}(\bar{1}10)$  and  $\text{InGaAsP}(\bar{1}10)$  on the composition of the  $\text{HBr}-\text{Br}_2-\text{H}_2\text{O}$  solution was investigated by using InGaAsP/InP multilayered structures grown by metallorganic chemical vapor deposition (MOCVD) on Sn-doped InP(001) wafers. The multilayered structure consisted of an InGaAsP MQW active layer ( $\lambda_g = 1.3 \mu\text{m}$ ), a p-InP cladding layer, and a p-InGaAsP capping layer. 1.5  $\mu\text{m}$  high mesas were fabricated by reactive ion etching with a  $\text{CH}_4/\text{H}_2/\text{O}_2$  gas mixture through  $\text{SiO}_2$  stripe masks arranged in the [110] direction. Figure 2 shows a cross-sectional image of the dry etching profile observed by scanning electron microscopy (SEM). HBr and  $\text{Br}_2$  concentrations were varied while keeping  $[\text{HBr}] + 100[\text{Br}_2] = 2.5 \text{ M}$ . Wet chemical etching was carried out at room temperature without stirring under ambient illumination. The etched depths perpendicular to the vertical mesa were then measured by SEM.

Epitaxial regrowth was carried out by MOCVD. Thin layers of InP were grown over the mesas so we could observe their structures. SEM and transmission electron microscopy (TEM) were used to characterize the regrowth profiles and defects at the interfaces. BHLDs fabricated using various  $\text{HBr}-\text{Br}_2-\text{H}_2\text{O}$  etchants were lifetime tested by operating them at a constant optical power output of 10 mW at 85°C.

## Results and Discussion

Figure 3 shows the etching rates of  $\text{InP}(\bar{1}10)$  and  $\text{In}_{0.76}\text{Ga}_{0.24}\text{As}_{0.55}\text{P}_{0.45}(\bar{1}10)$  ( $\lambda_g = 1.3 \mu\text{m}$ ) as a function of  $\text{HBr}-\text{Br}_2-\text{H}_2\text{O}$  concentration. Both rates showed a similar dependence on composition. Neither material dissolved in aqueous  $\text{Br}_2$ . The rates increased with HBr concentration and reached their respective maxima at HBr concentrations of about 0.4 M, and then decreased with a further increase in HBr concentration, which corresponds to a decrease in  $\text{Br}_2$  concentration. InP and InGaAsP were etched at almost the same rates in the concentration range from 0.30 M HBr/0.022 M  $\text{Br}_2$  to 0.50 M HBr/0.020 M  $\text{Br}_2$ . The morphology

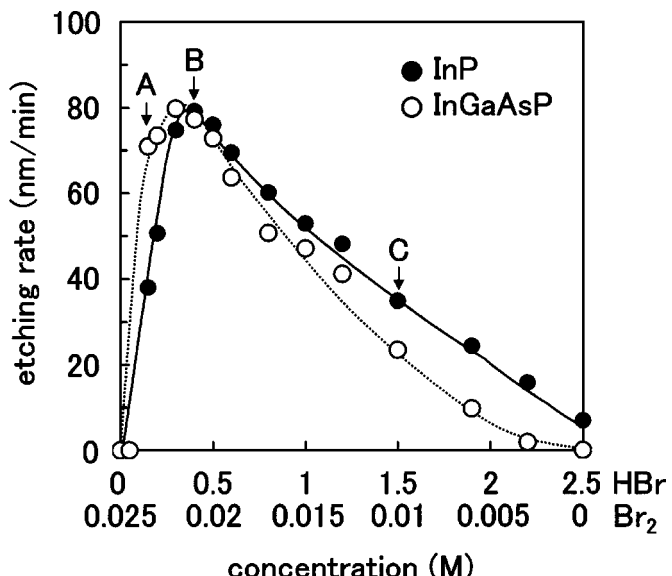


Figure 3. Etching rates of (●)  $\text{InP}(\bar{1}10)$  and (○)  $\text{InGaAsP}(\bar{1}10)$  as a function of HBr and  $\text{Br}_2$  concentrations.

of the etched surfaces was mirrorlike in most cases. However, etchants with very little HBr (from 0.025 M  $\text{Br}_2$  to 0.05 M HBr/0.0245 M  $\text{Br}_2$ ) produced rough surfaces. We also found that the etching rates by such low HBr etchants were not reproducible. These findings provide strong evidence that the dissolution of InP and InGaAsP in  $\text{HBr}-\text{Br}_2-\text{H}_2\text{O}$  solutions is mainly due to the dissolution of oxides, which requires both oxidizing agents and acids. The roughness produced by etchants with very little HBr may be due to the masking effects of residual oxide that remains on the surface because of insufficient acidity. It is clear that both materials hardly dissolved in either aqueous  $\text{Br}_2$  or aqueous HBr. However, InP would be etched substantially if the acidity of the solution were much higher than in our experiments.<sup>6</sup> This is because  $\text{InPO}_4$ , which is the most thermodynamically stable solid phase in the InP-H<sub>2</sub>O system, is no longer stable in a strongly acidic solution and tends to be reduced to produce  $\text{In}^{3+}$  plus  $\text{H}_3\text{PO}_4$ ,  $\text{In}^{3+}$  plus  $\text{H}_3\text{PO}_3$ , or  $\text{In}^{3+}$  plus  $\text{PH}_3$ , as depicted in the potential-pH diagram provided by Hsieh and Shih.<sup>7</sup> This explanation is consistent with the observation that InP was etched a little in aqueous HBr, which is much more acidic than aqueous  $\text{Br}_2$ . Profiles of the mesa walls etched by the particular solutions labeled A-C in Fig. 3 are discussed later.

Figure 4 shows the temperature dependence of the etching rate of InP(001) by 0.50 M HBr/0.020 M  $\text{Br}_2$ , which etches InP and InGaAsP at the same rate. The increase in rate on a logarithmic scale vs. temperature was insignificant and the activation energy was 0.14 eV. This low activation energy indicates that the etching reaction was diffusion controlled. If the etching rate had been controlled by the chemical reaction at the surfaces, the activation energy would have been much greater. Etching reactions with an activation energy greater than 0.4 eV are tentatively classified as kinetically controlled. Furthermore, the etched depth of about 80 nm observed after exposure for 1 min at 25°C leads us to think that the diffusing etchant species may have been  $\text{Br}_2$  molecules for the following reasons. Since the diffusion coefficient  $D$  of any chemical species in aqueous solutions at room temperature is of the order of  $1 \times 10^{-9} \text{ m}^2/\text{s}$ ,<sup>8,9</sup> the diffusion length  $\sqrt{4Dt}$  of the etchants over  $t = 1 \text{ min}$  is estimated to be around 500  $\mu\text{m}$ . Thus, roughly speaking, only the etchant within 500  $\mu\text{m}$  of the solid surfaces can reach

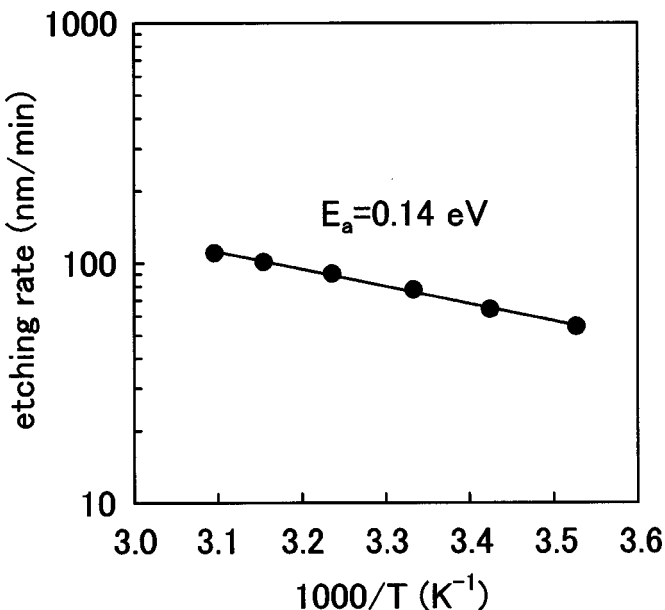


Figure 4. Temperature dependence of etching rate of InP(001).

them. Earlier studies revealed that  $\text{InPO}_4$  is the dominant oxidized state of InP after various treatments.<sup>7,10-13</sup> Thus, assuming that the oxidized state of InP is  $\text{InPO}_4$ , the redox reactions may be expressed as<sup>5,7</sup>



Since the standard redox potential of Reaction 2 (1.087 V) is higher than that of Reaction 1 (-0.385 V),  $\text{Br}_2$  can oxidize InP. Thus, these redox reactions can be merged into a single reaction

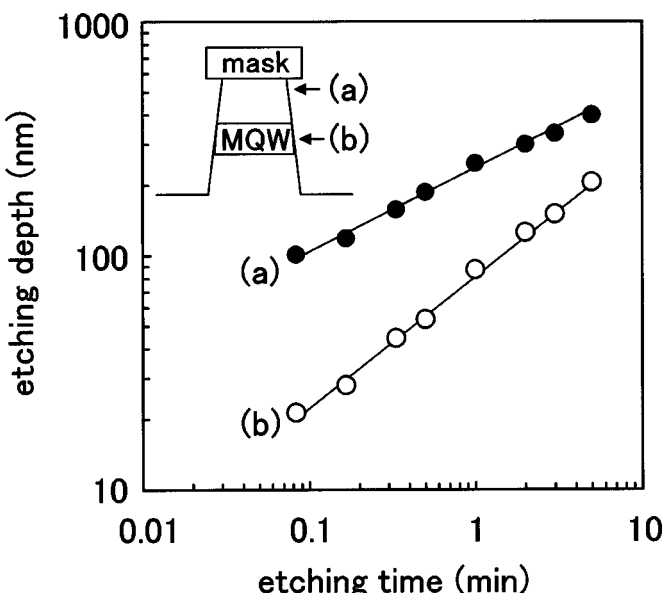


Figure 5. Depth of side etching at different positions as a function of etching time: (a) in the vicinity of the mask edge and (b) on the MQW active layer.

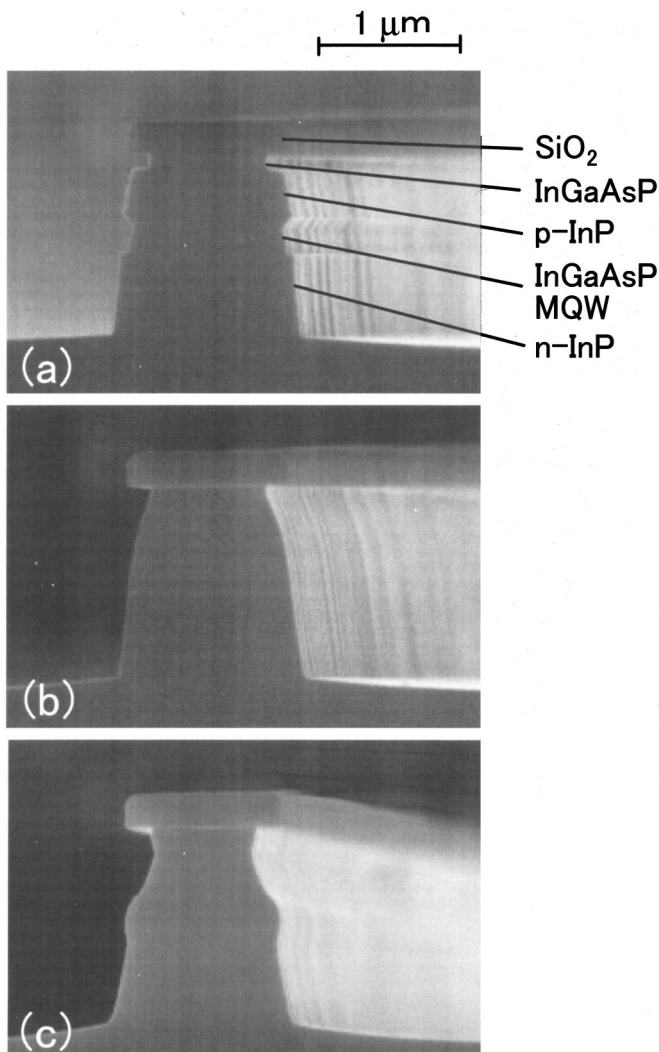


Figure 6. SEM cross sections of wall profiles formed by (a) etchant A, (b) etchant B, and (c) etchant C.

Therefore, four  $\text{Br}_2$  molecules are consumed in etching one InP molecule. The depth of etching ( $\delta$ ) by a purely diffusion-controlled etchant may be approximated by<sup>14</sup>

$$\delta = \frac{CM\sqrt{4Dt}}{N\rho} \quad [4]$$

where  $C$  is the concentration of the etchant,  $M$  is the mass of one molecule of the solid,  $N$  is the number of etchant molecules needed to remove one molecule from the solid, and  $\rho$  is the density of the solid. Thus, the etching depth of InP produced by exposure to 0.5 M HBr/0.02 M  $\text{Br}_2$  for 1 min is estimated to be about 80 nm. This estimate agrees well with the etching depths that we observed. On the other hand, if we consider that the rate-determining etchants are  $\text{Br}^-$  ions and assume that three  $\text{Br}^-$  ions are used in etching one InP molecule, then the etching depth can be estimated as 2.5  $\mu\text{m}$ , which is much greater than the observed depth. The large difference is mainly due to the difference in the concentration of the etchant species (0.5 M for HBr and 0.02 M for  $\text{Br}_2$ ). This argument indicates that the diffusion of  $\text{Br}_2$  molecules determines the etching rate.

In such diffusion-controlled etching, the presence of a mask is known to enhance etching in its vicinity. The etching rates are thus largest close to the mask edges and the distance from them has a strong effect on the depth of side etching.<sup>14,15</sup> This phenomenon

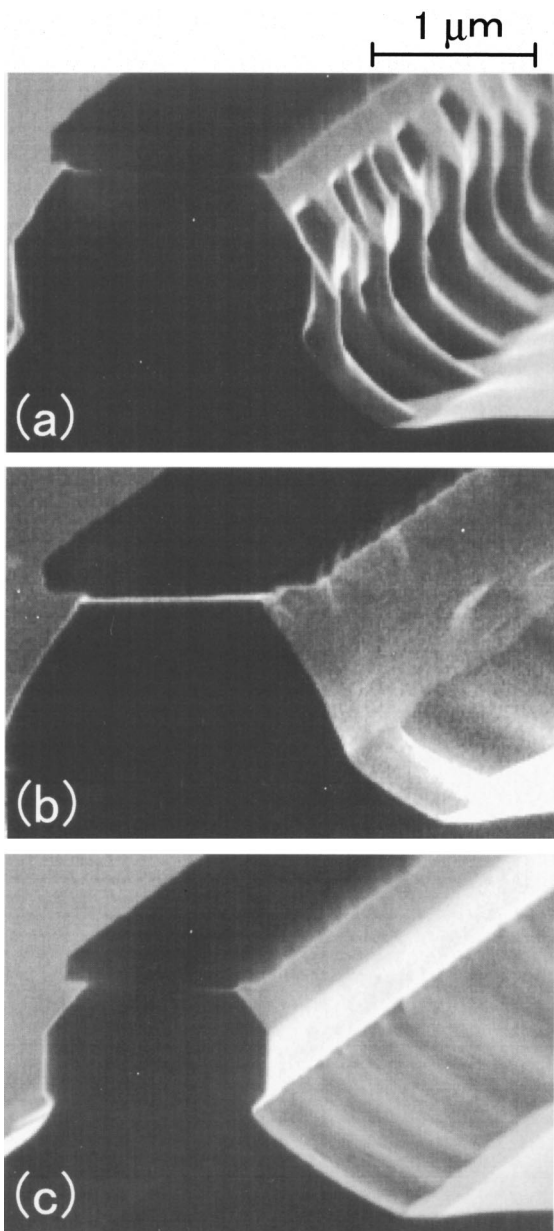


Figure 7. SEM cross sections of regrowth profiles formed using (a) etchant A, (b) etchant B, and (c) etchant C.

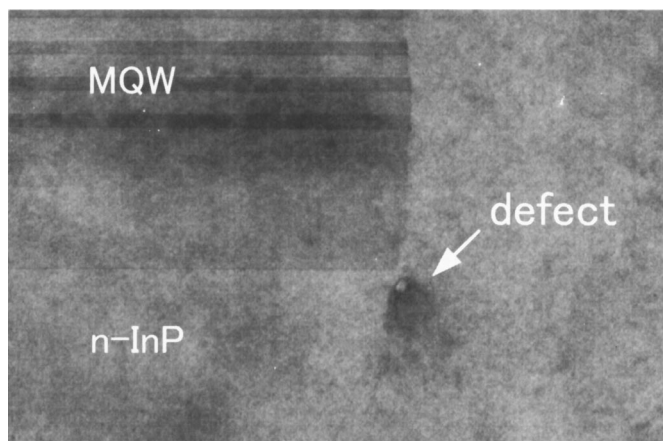


Figure 8. TEM image of an interface produced using etchant C, which causes rough sidewalls.

might cause uneven sidewalls. Figure 5 plots the depth of side etching immediately below the mask and at the MQW active layer. The slope of curve a is 0.35 (mask edge) while that of curve b is 0.59 (MQW active layer). Both slopes are reasonably close to the figure of 0.5 that would be expected for purely diffusion-controlled etching. This  $t^{1/2}$  dependence is expected for purely diffusion-controlled etching because only that portion of the etchant that is within the diffusion length  $\sqrt{4Dt}$  can reach the solid surface and etch the material. It is also clear, however, that etching at the mask edge shows a much weaker time dependence than etching of the MQW active layer. This tendency is consistent with the mathematical model of diffusion-controlled etching with convection that was presented by Kuiken *et al.*,<sup>14</sup> who obtained a  $t^{2/3}$  dependence at the mask edges and a  $t$  dependence at points far from them. The weaker time dependence is because there is a greater supply of fresh etchants in the vicinity of the mask. The lack of forced convection led to our results having a rather weaker time dependence than the results in the literature. The difference between the slopes of etched depth *vs.* time in Fig. 5 was found to cause rough sidewalls when the etching time was short, because of the large difference, at the beginning of etching, between the rates for the regions close to the mask edge and for the MQW active layer. However, the difference between the etching depths became less and less as time passed. Longer etching times are thus preferable from the viewpoint of producing smooth mesa sidewalls unless they cause the widths of the remaining mesa structures to become narrower than designed values.

On the basis of these findings, we tested several etchants on the dry-etched mesa structure. SEM cross sections of the mesa profiles produced by etchants of various compositions are shown in Fig. 6. The etching period was 1 min in each case. The mesa shape produced by the etchant with 0.15 M HBr/0.024 M Br<sub>2</sub> (etchant A) had recesses on each side of the MQW layer. This is because the etching rate of InGaAsP in etchant A was faster than that of InP as shown in Fig. 3. In contrast, the mesa shape produced by 1.5 M HBr/0.01 M Br<sub>2</sub> (etchant C) had a bump on each side of the MQW layer because the etching rate of InGaAsP in etchant C was slower than that of InP. The mesa profile produced by using the etchant with 0.5 M HBr/0.02 M Br<sub>2</sub> (etchant B) had smooth sidewalls because it etched the InP layers and InGaAsP layers at the same rate.

SEM images of regrowth profiles around mesas formed by using these three HBr-Br<sub>2</sub>-H<sub>2</sub>O solutions are shown in Fig. 7. Etchant B produced high quality regrowth interfaces with uniform growth around the mesa. Etchants A and C, on the other hand, formed nonuniform ones. When etchant A, which produced recesses in the MQW layer, was used, the regrowth profile became very rough because of the difference in growth rate from facet to facet of the sidewalls. When etchant C, which produced bumps at the side of the MQW layer, was used, (111)A planes appeared at the lower edges of the bumps on the side of the MQW active layer. The (111)A planes met curved growth faces like (11n) on the lower parts of the mesa sidewalls as they grew. Thus, some defects were formed in the vicinity of the lower edges of the bumps, as shown in the TEM image in Fig. 8.

Figure 9 shows the results of lifetime testing of BHLDs fabricated using etchants B and C. The change in operating currents,  $\Delta I_{op}/I_{op}$ , for BHLDs with smooth sidewalls fabricated using etchant B was 0.37% (from 0 to 2100 h at a constant 10 mW optical power output at 85°C), while the corresponding figure for BHLDs with rough sidewalls fabricated using etchant C was 3.0% on average. The change in driving currents was obtained by averaging over five samples for each type of BHLD. We thus conclude that smoother etching profiles improve the reliability of the BHLDs.

### Conclusions

We investigated the etching characteristics of InGaAsP/InP mesa structures in various HBr-Br<sub>2</sub>-H<sub>2</sub>O etchants. Our observations revealed an optimal concentration in the range from 0.30 M HBr/0.022 M Br<sub>2</sub> to 0.50 M HBr/0.020 M Br<sub>2</sub> that etches the InP(110)

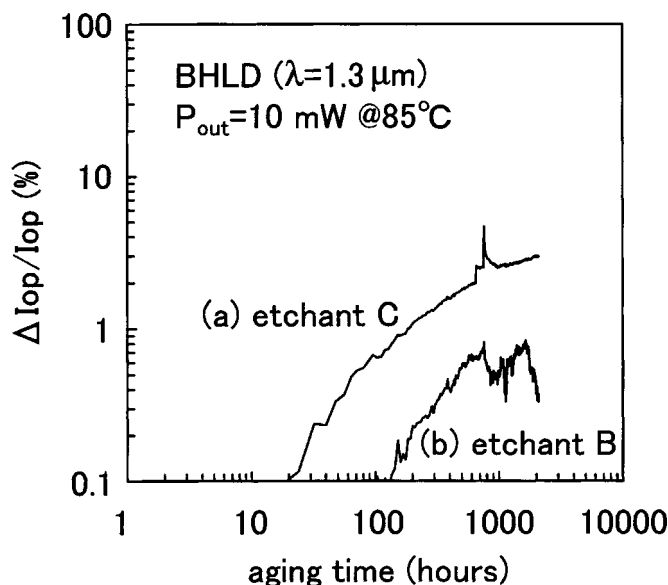


**Figure 9.** Lifetime-test results: BHLDs with mesa structures formed using (a) etchant C and (b) the optimal etchant B. (The BHLDs produced 10 mW of output power at 85°C.)

and InGaAsP(10) layers at the same rate. The etching mechanism is diffusion-controlled with an activation energy of 0.14 eV. We proposed a simple model of the etching process that can successfully

explain the observed etching characteristics. The etching rate was found to be controlled by the diffusion of the Br<sub>2</sub> molecules, which act as oxidizing agents. High-quality regrowth interfaces with fewer defects were formed on mesa sidewalls treated with the optimal etchant. The processing described in this paper results in a great improvement in the reliability of BHLDs.

Hitachi, Limited, assisted in meeting the publication costs of this article.

## References

1. H. Mawatari, M. Fukuda, S. Matsumoto, K. Kishi, and Y. Itaya, *J. Lightwave Technol.*, **15**, 534 (1997).
2. T. Chino, M. Ishino, M. Kito, and Y. Matsui, in *Proceedings of the 1998 International Conference on Indium Phosphide and Related Materials*, IEEE, p. 709, May 11-15, 1998.
3. R. Y. Fang, D. Bertone, G. Morello, and M. Meliga, *J. Electrochem. Soc.*, **144**, 3940 (1997).
4. S. Adachi, Y. Noguchi, and H. Kawaguchi, *J. Electrochem. Soc.*, **129**, 1053 (1982).
5. A. J. Bard, R. Parsons, and J. Jordan, *Standard Potentials in Aqueous Solution*, Marcel Dekker, Inc., New York (1985).
6. P. H. L. Notten and A. A. J. M. Damen, *Appl. Surf. Sci.*, **28**, 331 (1987).
7. H. F. Hsieh and H. C. Shih, *J. Electrochem. Soc.*, **137**, 1348 (1990).
8. D. M. Himmelblau, *Chem. Rev.*, **64**, 527 (1964).
9. R. H. Stokes, *J. Am. Chem. Soc.*, **72**, 2243 (1950).
10. J. F. Wager, D. L. Ellsworth, S. M. Goodnick, and C. W. Wilmsen, *J. Vac. Sci. Technol.*, **19**, 513 (1981).
11. J. F. Wager, K. M. Geib, C. W. Wilmsen, and L. L. Kazmerski, *J. Vac. Sci. Technol. B*, **1**, 778 (1983).
12. A. Gnivarc'h, H. L'Haridon, G. Pelous, G. Hollinger, and P. Pertosa, *J. Appl. Phys.*, **55**, 1139 (1984).
13. G. Hollinger and E. Bergignat, *J. Vac. Sci. Technol. A*, **3**, 2082 (1985).
14. H. K. Kuiken, J. J. Kelly, and P. H. L. Notten, *J. Electrochem. Soc.*, **133**, 1217 (1986).
15. P. H. L. Notten, J. J. Kelly, and H. K. Kuiken, *J. Electrochem. Soc.*, **133**, 1226 (1986).